Study of Kuroshio Intrusion and Transport using Moorings and EM-APEX Floats in QPEU Experiment

Ren-Chieh Lien
Applied Physics Laboratory
University of Washington
1013 NE 40th Street
Seattle, Washington 98105
Phone: (206) 685-1079 fax: (206) 543-6785 email: lien@apl.washington.edu

Thomas B. Sanford
Applied Physics Laboratory and School of Oceanography
University of Washington
1013 NE 40th Street
Seattle, Washington 98105
Phone: (206) 685-1365 fax: (206) 543-6785 email: sanford@apl.washington.edu

Award Number: N00014-08-1-0558

LONG-TERM GOALS

Our long-term scientific goals are to understand the dynamics and identify mechanisms of small-scale processes in the ocean with the objective of developing improved parameterizations of mixing for ocean models. Internal tides, inertial waves, nonlinear internal waves (NLIWs), and turbulence mixing are all key components to understanding mixing within the stratified ocean. Each of these factors can lead to uncertainty within current ocean models due to their complex interplay. This study focuses primarily on small-scale processes, internal tides, and also key circulation features including cold dome events localized at the continental slope of the East China Sea (ECS) and intrusions generated as the Kuroshio and barotropic tides interact with the continental shelf of the ECS. These small-scale processes and circulation features modulate the temporal, horizontal, and vertical spatial structures of the water properties of the ocean. These processes may significantly modify acoustic properties and thus introduce uncertainty into sonar performance and acoustic propagation models. Our ultimate goal is to collaborate with acousticians to identify oceanic processes that alter acoustic properties. A detailed understanding of these properties, mechanism, and dynamics will aid in quantification and assessment of uncertainty in acoustic prediction.

OBJECTIVES

The primary objective of this observational program is the quantification of oceanic physical properties and velocity structure including temporal and spatial structures and their relation to unique processes in the ECS region. The objectives are to quantify and to understand the dynamics of the Kuroshio intrusion and its migration into the southern East China Sea (SECS), to identify the generation mechanisms of the Cold Dome often found on the SECS, to quantify NLIWs and their statistical

properties in the SECS, to quantify the internal tidal energy flux in the SECS, to study the effects of the Kuroshio front on the internal tidal energy flux, and to provide our results to acoustic investigators to assess the uncertainty in acoustic prediction.

APPROACH

An observational field program was conducted as part of an integrated observational program. Our contribution to the integrated program included two observational components, an array of six subsurface moorings and an array of six EM-APEX profiling floats. Six subsurface moorings were deployed off the eastern and northeastern coast of Taiwan 5 August through 12 September 2009; five were located near North Mien Hua Canyon (NMHC) (QP2 – QP6) and one on the I-Lan Ridge (QP1) as part of the extended observational program (Fig. 1). These moorings included 75-kHz Long Ranger ADCPs and a series of temperature/conductivity sensors. The mooring observations are used to quantify the Kuroshio intrusion and migration, internal tidal energy and energy flux, NLIWs and the Cold Dome feature. The EM-APEX floats were deployed from 23 August through 6 September 2009 for a half-month intensive observational period that overlapped with the final half month of the mooring deployments. Six EM-APEX floats were deployed into the North Mien-Hua Canyon and allowed to drift southwest to the operational boundary. At that point they were retrieved and redeployed into North Mien-Hua Canyon. The six EM-APEX floats were deployed a total of 16 times and completed 395 vertical profiles. The floats provided near real-time observations of velocity, temperature, and salinity.

WORK COMPLETED

We focused our analysis on Kuroshio intrusions and internal waves in the East China Sea. Kevin Taylor, a graduate student, studied the Kuroshio intrusion into the East China Sea following the passage of Typhoon Morakot. He obtained his Master's degree in 2012. Two papers have been published and two papers are in press. Some significant results of our work are summarized in the following section.

RESULTS

Kuroshio Intrusion

Two robust intrusions of the Kuroshio appeared on the ECS slope during August 2009; their signature was an abnormally high salinity of 34.6 psu averaged between the1024 kg m^{-3} and 1026 kg m^{-3} isopycnals, characteristic of Kuroshio subsurface water (Fig. 2a). The average was computed between density surfaces to avoid the effect of the large vertical isopycnal heaving associated with the semi-diurnal internal tides in the region. Vertical displacements of isopycnals due to internal tides on the order of +/–50 m were observed; some reached amplitudes greater than 100 m. The velocity fluctuation of semidiurnal internal tides was as large as 0.5 m s^{-1}. The density range 1024–1026 kg m^{-3} was covered consistently by the mooring CTD observations and equated to a mean depth range of 75–270 m for the typical ECS slope water (Fig. 2d). The T/S property at the most southern mooring on I-Lan Ridge revealed first the shallow Kuroshio water (~1023 kg m^{-3}) then deep Kuroshio water (>1024 kg m^{-3}) during 6–15 August (Fig. 2c, red dots).

The largest intrusion was observed in conjunction with Typhoon Morakot (Fig. 2b). A large increase of salinity was observed at the most southern mooring during the evening of 8 August 2009. This was

less than one day after Morakot made landfall at Taiwan on 7 August. The large positive salinity anomaly traveled northward through the mooring array at a speed of ~0.8 m s^{-1} (Fig. 2a), which is the speed of the main path of the Kuroshio at a depth of 104 m (Tang et al., 1999). This may suggest that Typhoon Morakot caused the Kuroshio velocity core to meander towards shallower waters. The salinity anomaly persisted longest at the northernmost mooring (Fig. 2a, mooring QP6, blue salinity record). The intrusion observed by the mooring array was likely partially due to a meander of the main velocity core of the Kuroshio as well as to an intrusion from a branch of the Kuroshio onto the ECS slope.

Concurrent AVISO altimetry data show a change of the absolute geostrophic sea surface velocity in the region of NMHC shifted from northeast to north just after Typhoon Morakot transited through the region. The shift of the absolute geostrophic velocity to north at NMHC supports our observations of increased salinity due to an intrusion of the Kuroshio. A possible explanation for the shelfward movement of the Kuroshio and a northward shift in geostrophic velocity may be attributed to coastal upwelling caused by Typhoon Morakot winds. Southerly winds due to the passage of Typhoon Hai-Tang in the region during the summer of 2005 were suggested to have created coastal upwelling east of Taiwan (Morimoto et al., 2009). The upwelling generated an east–west sea level difference, which in turn generated a northward geostrophic current. The resultant flow could have pushed the Kuroshio towards the ECS shelf (Morimoto et al., 2009).

Internal Tides

The primary generation sites of semidiurnal internal tides on the ECS are identified, using the critical slope analysis, as (1) along the shelf break north of the head of NMHC, (2) a broad area west of moorings QP2 and QP6, and (3) a narrow area south of the QP2 mooring (Fig. 3). The strongest generation site for the semidiurnal internal tide is expected at (2) because of its broad area and stronger barotropic tide. Internal tidal beams generated at the continental shelf break propagating past mooring QP2 compare well with the tidal beams obtained from a Princeton Ocean Model (POM) simulation (Fig. 4).

The temporal variation of depth integrated horizontal kinetic energy of semidiurnal internal tides is shown in Fig. 5. Both the total and low-wavenumber components, using a low-pass filter at the half-power point of a 300-m vertical scale, are the strongest at mooring QP6, near the head of NMHC, and the weakest at mooring QP3, furthest away from the generation sites. The high-wavenumber horizontal kinetic energy shows less variability among moorings. All of the total, low-wavenumber, and high-wavenumber horizontal kinetic energy exhibit a fortnightly cycle, in close unison with the barotropic tides (Fig. 5a).

Layers of spatially coherent strong vertical shear, associated with high-wavenumber semidiurnal internal tides, were observed by moorings, EM-APEX floats, and shipboard ADCP. To investigate the vertical propagation of high-wavenumber semidiurnal internal tides, we decomposed the observed velocity into upward and downward propagating waves. Decomposition results of observations on 24 – 27 August are illustrated in Fig. 6. The observed velocity field is first band-pass filtered at the semidiurnal tidal frequency band, at 6–18-hr period. The semidiurnal tidal velocity is WKB normalized, and the vertical scale is WKB stretched. We further separate the low-wavenumber internal tides, vertical scales > 300 m, from the high-wavenumber internal tides, vertical scales < 300 m) (Fig. 6b and 6c). High-wavenumber internal tides are decomposed into components of upward and

downward energy propagation (Fig. 6d and 6e). Several distinct features are revealed. Some are common features for the entire experimental period, but some are unique to this particular 3-day period. Low-wavenumber internal tides have stronger energy than high-wavenumber internal tides and exhibit predominant upward phase propagation. The high-wavenumber internal tide has a complex temporal-spatial pattern, consisting of both upward and downward propagating waves. The superposition of upward and downward propagation waves of high-wavenumber internal tides results in patches of enhanced energy of ~50-m scales.

We compute the semidiurnal internal tidal energy flux from EM-APEX float observations following the method described by Kunze et al. (2002). EM-APEX floats were deployed in five groups (A–E) of three or four floats each (Fig. 7a). The magnitude of internal tidal energy flux increases from group B to group E, following the increase of barotropic tidal forcing. Group A was deployed during the end of spring tide and the tidal energy flux shows the strongest spatial variation in magnitude and direction, 0 –10 kW m^{-1}. Note that EM-APEX observations were taken during weak barotropic tidal forcing. Averaging all estimates of depth-integrated internal tidal energy flux, the zonal component is 1.3 (±1.3) kW m^{-1}, and the meridional component is –0.3 (±2.5) kW m^{-1}, where the value within the parentheses represents one standard deviation. The standard deviation indicates the temporal and spatial variability of the flux.

The POM (Blumberg and Mellor, 1987) is used to simulate semidiurnal internal tides in the ECS. Two model runs are performed using two different initial T/S profiles. The run with the "normal" (T, S) profile is termed M2 and the run with the post-Typhoon Morakot (T, S) profile is termed M2a. The model semidiurnal internal tidal energy flux varies greatly by the initial TS profiles (Fig. 8). The M_2 internal tidal energy flux is ~5 kW m^{-1} southeastward or southward in the North Mien-Hua Canyon region and is 5–8 kW m^{-1} emanating northeastward from the I-Lan Ridge. The southeastward energy beam emanating from the North Mien-Hua Canyon is stronger in the M2a run than in the M2 run, whereas the northeastward energy beam from the I-Lan Ridge is stronger in the M2 run than in the M2a run. The modeled magnitude of the internal tidal energy flux at mooring sites varies between 1.0 and 7.2 kW m^{-1}, is predominantly seaward, and is the strongest at QP4. These features agree qualitatively with observations. However, model results of the magnitude and direction of internal tidal energy flux at individual moorings differ significantly from those of observations. The discrepancy between the modeled and observational results may be due to the lack of the S_2 tidal forcing, the use of different stratification profiles, the absence of mesoscale processes in the model, insufficient model and bathymetry resolutions, or an inaccurate sub-grid parameterization scheme.

IMPACT/APPLICATION

In-situ observations and model results conclude that strong internal tides exist on the continental slope of the ECS. Vertical displacements of internal tides on the order of +/–50 m were observed; some reached amplitudes greater than 100 m. Two robust intrusions of the Kuroshio appeared on the ECS slope during August 2009. The strongest intrusion was observed in conjunction with Typhoon Morakot. Spatially coherent shear layers associated with high-wavenumber semidiurnal internal tides are present on the ECS continental slope. Internal tidal energy flux varies between 3.0 and 10.7 kW m^{-1}, computed from mooring measurements. Observed total energy in the internal wave continuum is 6.2–13.3 times the open ocean value. To quantify, predict, and exploit the uncertainty of acoustic propagation and sonar performance, we need to understand the dynamics of these oceanic processes and their effects on the sound speed.

RELATED PROJECTS

Process Study of Oceanic Responses to Typhoons using Arrays of EM-APEX Floats and Moorings (N00014-08-1-0560) as a part of ITOP DRI: We study the dynamics of the oceanic response to and recovery from tropical cyclones in the western Pacific using long-term mooring observations and an array of EM-APEX floats. Pacific typhoons may cause cold pools on the continental shelf of the East China Sea. The cold pool dynamics are likely related to the Kuroshio and its intrusion as well as the shelf/slope oceanic processes. The cold pool could produce a significant acoustic anomaly that is the focus of the present project.

REFERENCES

Blumberg, A. F. and G. F. Mellor. 1987. A description of a three dimensional coastal ocean circulation model, *in* Three-Dimensional Coastal Ocean Models, Coastal and Estuarine Sciences, vol. 4, N. Heaps, ed., AGU, Washington D.C., 1-16.

Jan, S., J. Wang, Y. J. Yang, C.-C. Hung, C.-S. Chern, G. Gawarkiewicz, R.-C. Lien, L. Centurioni, J.-Y. Kuo, and B. Wang. 2013. Observation of Typhoon Morakot-induced freshwater pulse off northern Taiwan in August 2009. *Journal of Marine Research*, in press.

Kunze, E., L. K. Rosenfeld, G. S. Carter, and M. C. Gregg. 2002. Internal waves in Monterey Submarine Canyon. *Journal of Physical Oceanography*, 32, 1890–1913.

Morimoto, A., S. Kojima, S. Jan and D. Takahashi. 2009. Movement of the Kuroshio axis to the northeast shelf of Taiwan during typhoon events. *Estuarine, Coastal and Shelf Science* 82, 547-552.

Tang, T. Y., Y. Hsueh, Y. J. Yang and J. C. Ma. 1999. Continental slope flow northeast of Taiwan. *Journal of Physical Oceanography* 29, 1353-1362.

PUBLICATIONS

Lien, R.-C., T. B. Sanford, S. Jan, M.-H. Chang, and B. B. Ma. 2013. Internal tides on the East China Sea continental slope. *Journal of Marine Research*, in press.

Jan, S., J. Wang, Y. J. Yang, C.-C. Hung, C.-S. Chern, G. Gawarkiewicz, R.-C. Lien, L. Centurioni, J.-Y. Kuo, and B. Wang. 2013. Observation of Typhoon Morakot-induced freshwater pulse off northern Taiwan in August 2009. *Journal of Marine Research*, in press.

Jan, S., C.-C. Chen, Y.-L. Tsai, Y. J. Yang, C. S. Chern, G. Gawarkiewicz, R.-C. Lien, L. Centurioni, and J.-Y. Kuo. 2011. Mean structure and variability of the cold dome northeast of Taiwan, *Oceanography*, 24, 100-109.

Gawarkiewicz, G. et al. 2011. Can we accurately predict circulation and internal waves northeast of Taiwan? Chasing uncertainty in the Cold Dome. *Oceanography*, 24, 110-121.

HONORS/AWARDS/PRIZES

Gledden Sr. Visiting Fellowship at U. Western Australia (Sanford, October 2008).

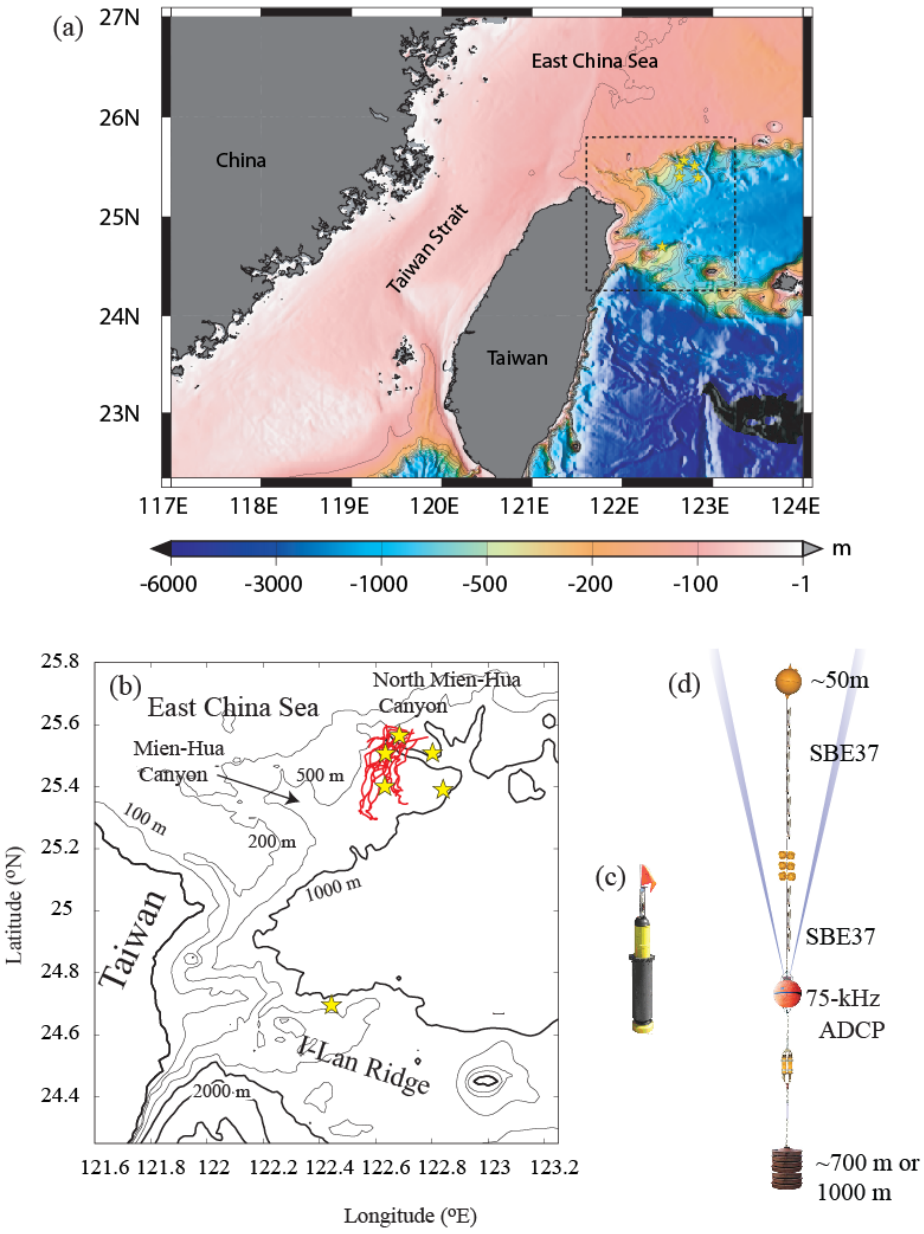

Figure 1: (a) Bathymetry chart surrounding Taiwan, (b) bathymetry detail from within the dashed rectangle in (a). The 500-m resolution bathymetric data were provided by the Ocean Data Bank of Taiwan's National Science Council. Thick black curves are isobaths with 1000-m interval. Thin black curves are isobaths of 100, 200, and 500 m. Yellow stars represent mooring positions. Red curves represent trajectories of EM-APEX floats. (c) Photo of EM-APEX float. (d) Mooring configuration.

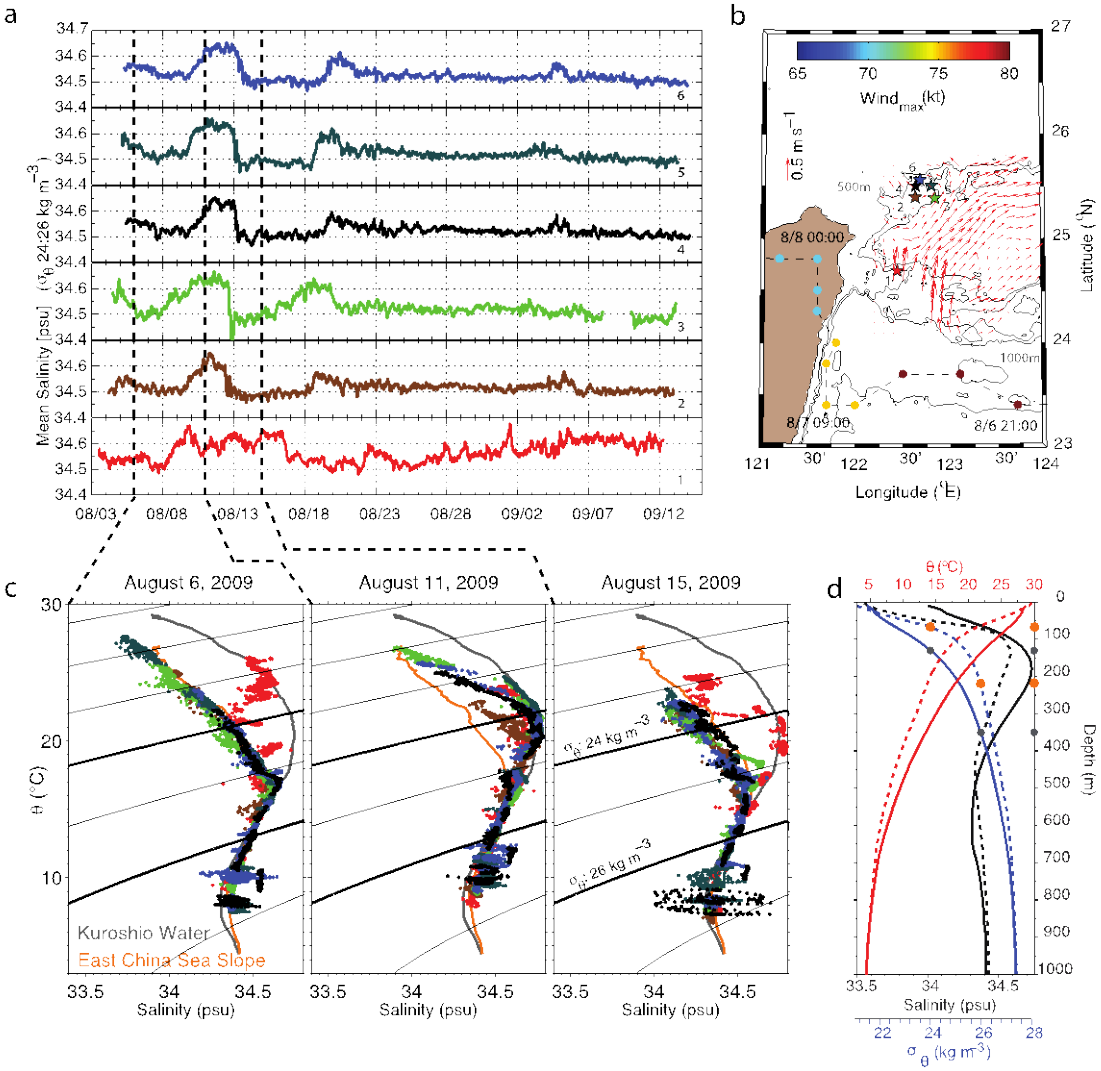

Figure 2. (a) Temporal variation of salinity averaged between σ_θ 24 kg m^{-3} and 26 kg m^{-3} at six moorings deployed east and northeast of Taiwan. (b) Horizontal velocity averaged from the sea surface to either the bottom or 1000 m depth from gliders in 0.1° latitude × 0.1° longitude grid points (red velocity arrows), Typhoon Morakot track and maximum wind speed (filled circles color-coded by maximum wind speed), and six mooring locations (colored stars) that are color-coded and numbered to correspond to mean salinity records in (a). (c) Potential temperature and salinity plot before Typhoon Morakot (left), immediately after Typhoon Morakot (center), and several days after Typhoon Morakot (right). Colored dots correspond with color-coding of moorings (b, stars) and mean salinity records (a). Kuroshio T/S property (solid gray line) was collected from gliders; East China Sea slope water T/S property (solid orange line) was collected from EM-APEX floats. (d) Average vertical profile of salinity (black), potential temperature (red), and potential density (blue) for the Kuroshio collected by gliders in Okinawa Trough (solid lines) and the East China Sea slope collected by EM-APEX floats (dashed lines). Average depth associated with σ_θ = 24 kg m^{-3} and 26 kg m^{-3} for the Kuroshio (gray) and the East China Sea Slope (orange) are shown with colored circles.

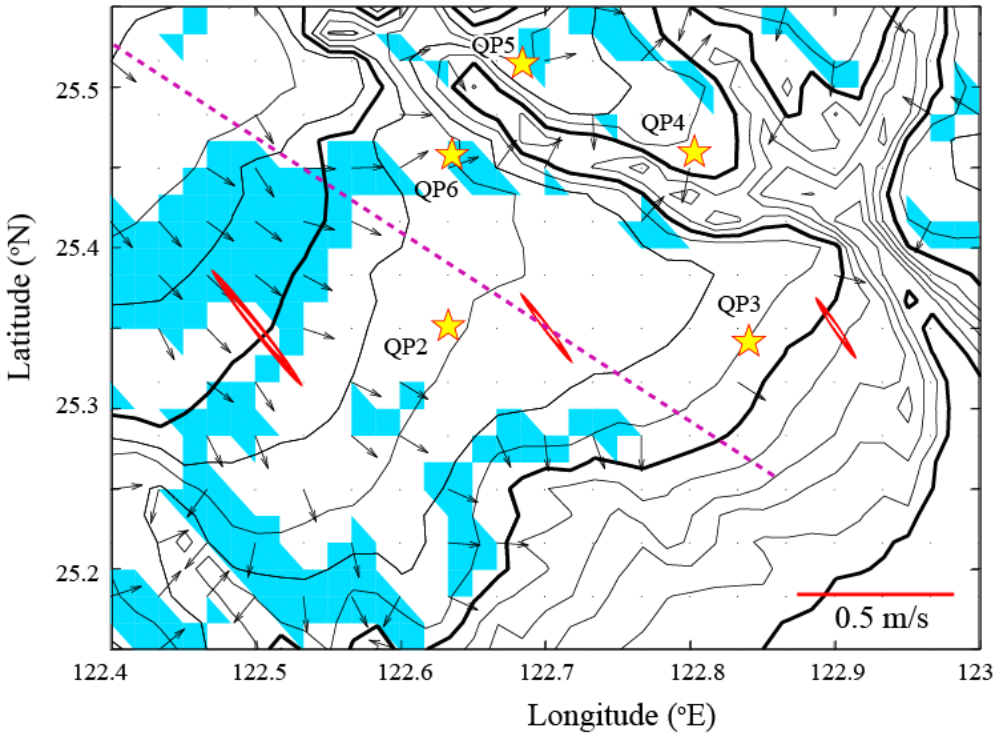

Figure 3: The critical slope regions (cyan shading), slope gradient (arrows), and locations of five moorings (stars). Three red ellipses are barotropic tidal current ellipses computed from the Oregon State University TOPEX/Poseidon Global Inverse Solution (TPXO). The magenta dashed line indicates the section shown in Figure 4. The horizontal red line shows the velocity scale of 0.5 m s^{-1}.

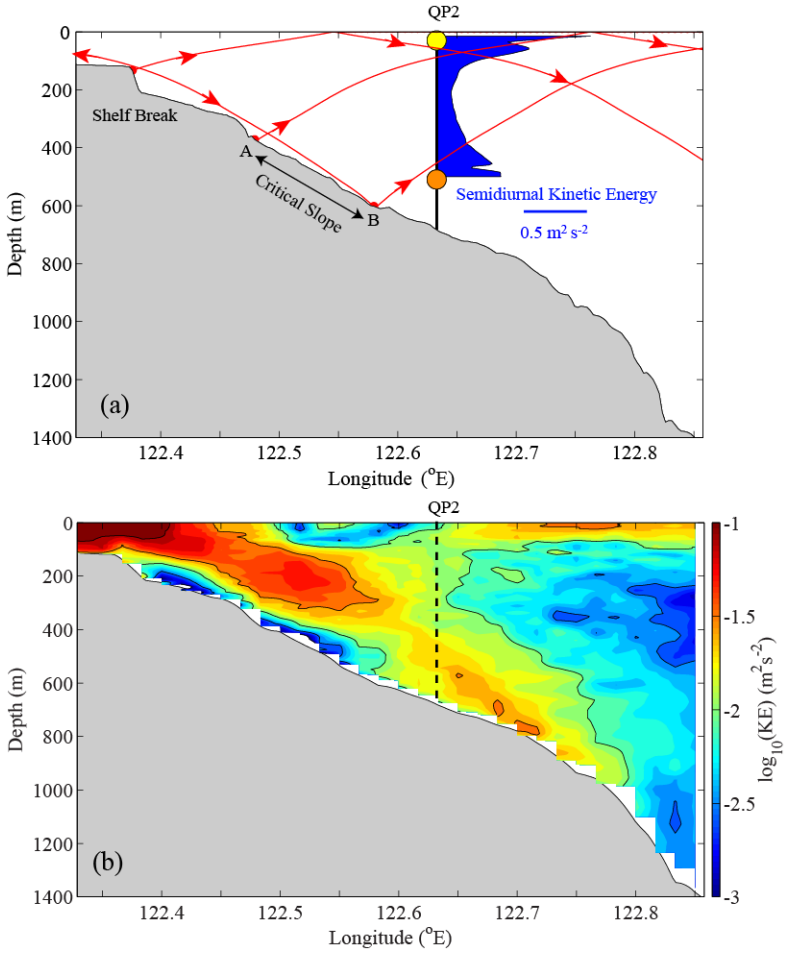

Figure 4: (a) Illustration of characteristics of internal tides generated at the shelf break and bouncing off the critical sloping bottom and off the sea surface, and generated at the critical slope (red curves) along the section shown as the magenta dashed line in Fig. 3. They are computed using stratification observed from EM-APEX floats. The blue shading shows the semidiurnal tidal kinetic energy observed at mooring QP2. The brown and yellow dots represent the two subsurface floats of the mooring. The scale of kinetic energy of 0.5 $m^2 s^{-2}$ is shown. (b) A snapshot of POM model results of the horizontal kinetic energy of the M_2 semidiurnal tide along the same section. The vertical dashed line indicates the location of mooring QP2.

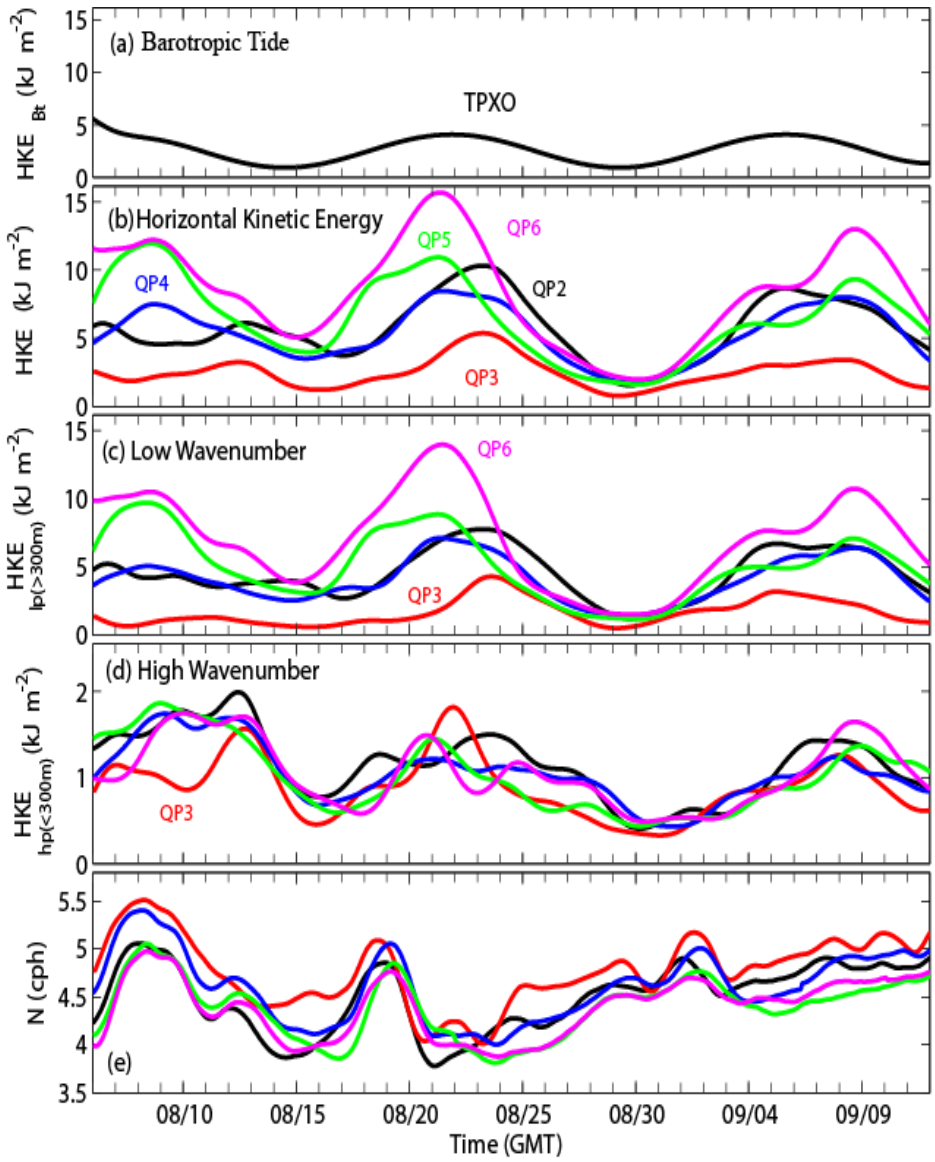

Figure 5: Temporal variations of (a) depth integrated horizontal kinetic energy of semidiurnal barotropic tide computed from TPXO, (b) depth integrated horizontal kinetic energy for semidiurnal internal tides, (c) similar to (b) but for vertical scales greater than 300 m (low wavenumber), and (d) similar to (b) but for vertical scales less than 300 m (high wavenumber). (e) Temporal variations of the depth averaged stratifications.

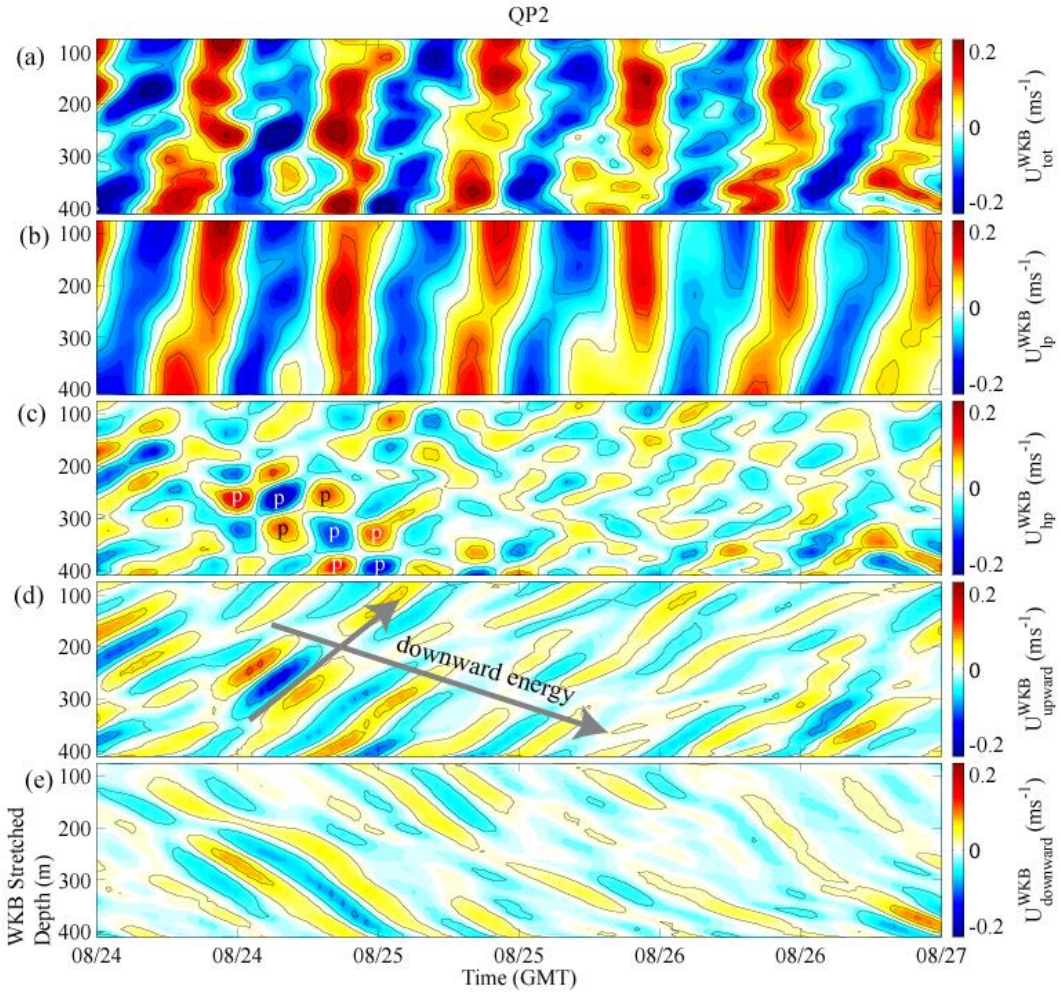

Figure 6: Decomposition of upward and downward propagation waves at QP2. (a) WKB-scaled zonal velocity component band-pass filtered in the semidiurnal tidal period in the WKB stretched vertical coordinate. (b) Zonal velocity low-pass filtered (low wavenumber) with vertical scales greater than 300 m, and (c) zonal velocity with vertical scales less than 300 m (high wavenumber). (d) and (e) Decomposition of high vertical-wavenumber velocity in (c) into the upward phase propagation and downward phase propagation, respectively. Two gray arrows in (d) represent the downward energy propagation, and the upward phase propagation of internal tidal energy. Patches in (c) labeled 'p' represent the intensification of high vertical-wavenumber velocity due to the superposition of upward and downward propagation waves.

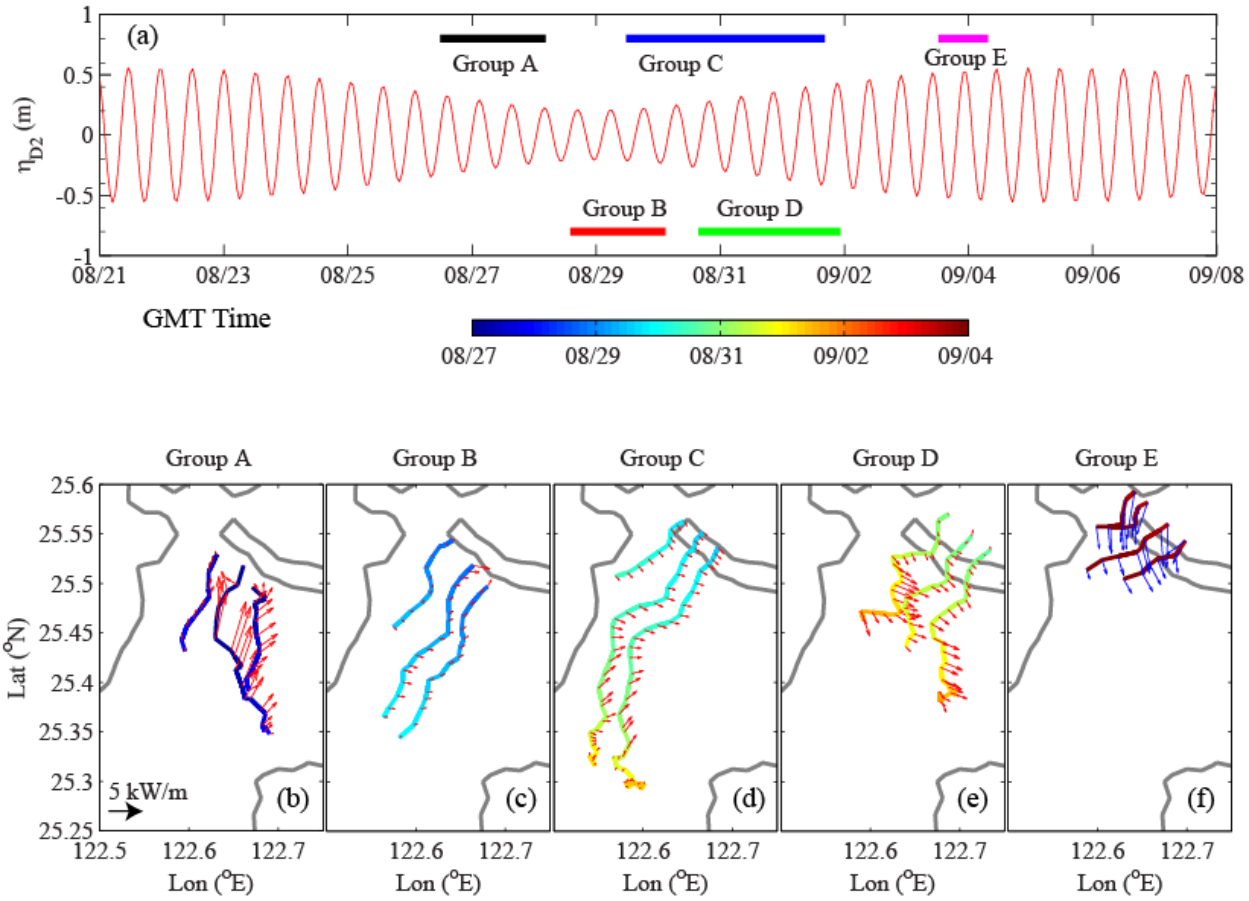

Figure 7: (a) TPXO predicted semidiurnal barotropic tidal elevation, and (b)–(f) the depth integrated semidiurnal internal tidal energy flux (red arrows) along trajectories of EM-APEX floats. EM-APEX floats were deployed in five groups (A–E), each with three or four floats. Colors along the trajectories represent the time, corresponding to the horizontal color bar. The reference scale of 5 kW m^{-1} is shown on panel (b). Gray curves in panels (b)–(f) are isobaths of 500 m, 1000 m, and 1500 m.

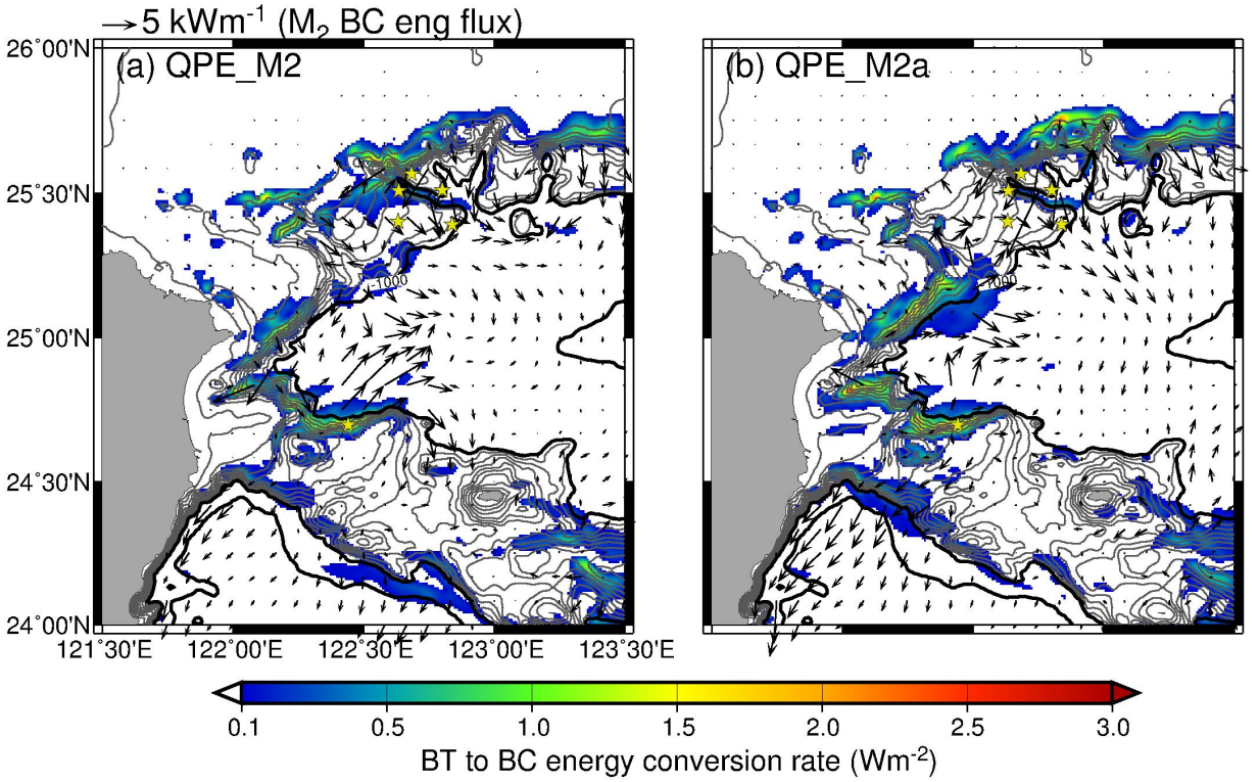

Figure 8: Time averaged and depth-integrated rate of barotropic to baroclinic energy conversion (color shading) and energy flux (arrows) for modeled M_2 internal tides. (a) The results of model run1 (M2a), and (b) the results of model run2 (M2). Yellow stars mark the mooring locations. The scale of the energy flux of 5 kW m^{-1} is shown on top of (a).

REPORT DOCUMENTATION PAGE

Form Approved
OMB No. 0704-0188

1. REPORT DATE *(DD-MM-YYYY)*	2. REPORT TYPE	3. DATES COVERED *(From - To)*
06/27/2013	Final Report	3/1/08 - 2/28/13

4. TITLE AND SUBTITLE
Study of Kuroshio Intrusion and Transport using Moorings and EM-APEX Floats in QPEU Experiment

5a. CONTRACT NUMBER

5b. GRANT NUMBER
N00014-08-1-0558

5c. PROGRAM ELEMENT NUMBER

6. AUTHOR(S)
Ren-Chieh Lien and Thomas B. Sanford

5d. PROJECT NUMBER

5e. TASK NUMBER

5f. WORK UNIT NUMBER

7. PERFORMING ORGANIZATION NAME(S) AND ADDRESS(ES)
Applied Physics Laboratory
University of Washington
1014 NE 40th Street
Seattle, WA 98105

8. PERFORMING ORGANIZATION REPORT NUMBER

9. SPONSORING/MONITORING AGENCY NAME(S) AND ADDRESS(ES)
Theresa Paluszkiewicz, Code ONR 322
Office of Naval Research
875 North Randolph Street
Arlington, VA 22203-1995

10. SPONSOR/MONITOR'S ACRONYM(S)

11. SPONSOR/MONITOR'S REPORT NUMBER(S)

12. DISTRIBUTION/AVAILABILITY STATEMENT
Approved for public release; distribution is unlimited.

13. SUPPLEMENTARY NOTES

14. ABSTRACT
The objectives are to quantify and to understand the dynamics of the Kuroshio intrusion and its migration into the southern East China Sea (SECS), to identify the generation mechanisms of the Cold Dome often found on the SECS, to quantify NLIWs and their statistical properties in the SECS, to quantify the internal tidal energy flux in the SECS, to study the effects of the Kuroshio front on the internal tidal energy flux, and to provide our results to acoustic investigators to assess the uncertainty in acoustic prediction.

15. SUBJECT TERMS

16. SECURITY CLASSIFICATION OF:			17. LIMITATION OF ABSTRACT	18. NUMBER OF PAGES	19a. NAME OF RESPONSIBLE PERSON
a. REPORT	b. ABSTRACT	c. THIS PAGE			Ren-Chieh Lien
U	U	U	UU	14	19b. TELEPHONE NUMBER *(Include area code)* (206) 685-1079